FULLY BLACK AND RELIABLE PV MODULES WITH A COST-EFFECTIVE INKJET COATING OF CELL STRINGS

[1]Christian H. Schiller, [1]Stephan Hoffmann, [1]Mike Jahn, [1]Angela De Rose, [1,*]Martin Heinrich

[1] Fraunhofer Institute for Solar Energy Systems ISE,
Freiburg, Germany, Heidenhofstraße 2, 79110 Freiburg i.Br., Germany

[*]Corresponding author, e-mail to: martin.heinrich@ise.fraunhofer.de

ABSTRACT: The energy transition requires a massive expansion of photovoltaics (PV) on all available areas in the next few years. For integrative photovoltaic applications (XIPV), an aesthetically appealing PV module design for acceptance and a high photoconversion efficiency are desirable. To achieve this goal using common PERC solar cells with five-busbar interconnection, we present an inkjet process that complies with the speed of industrial stringers to blacken the cell connectors after soldering, resulting in an unaffected homogeneous black impression. The optical impression of our manufactured PV modules remains intact after extended (400 temperature cycles (TC), 120 kWh/m^2 ultraviolet radiation (UV), 2000 h damp heat (DH) exposure) and combined (UV-DH, UV-DH+TC) climate chamber tests following IEC standards. The power loss due to printing on cell connectors is 1.4 % compared to PV modules without blackened cell connectors.

Keywords: Inkjet printing, cell strings, integrated PV, black PV modules, ribbons

1 INTRODUCTION

Since 1974 the limits to growth are evident and the discussion on a sustainable future of humanity has emerged [1]. To ensure peaceful human coexistence, we simply must limit the global temperature increase to 1.5 °C. The global economy must be decarbonized. This requires redirecting billions of dollars of global financial flows into sustainable investments (economically efficient, socially just, ecologically sustainable) [2]. As stated specifically in Agenda 2030 [3]: the 7th goal of sustainable development is to ensure access to affordable, reliable, sustainable and modern energy for all [3].

This energy revolution requires a strong expansion of photovoltaics in the next few years [4]. All available areas must be used for this purpose. Photovoltaics shall be integrated in vehicles and on buildings. It may solve land use conflicts in combination with agriculture, water areas and traffic routes [5].

To integrate photovoltaic (PV) modules in façades of buildings or other applications (cars, etc.), it is usually inevitable to achieve an aesthetically pleasing and appealing design for acceptance [6, 7]. In addition to the individual colouring of PV modules as façade elements, the homogeneous appearance for all angles of view and a high photoconversion efficiency are desirable [8]. To achieve this, one approach for coloured PV modules was shown by Bläsi *et al.* whose MorphoColor concept allows the same optical impression from different viewing angles on a PV module [8]. Even for stone façades, a visually appealing proposition was shown to integrate PV modules unobtrusively, however, with some limitations of photoconversion efficiency [9]. Another approach is to use PV modules with the matrix shingle technology that offers a cell interconnection without ribbons, wires or space between cell strings and hence without metallic reflections [10]. However, PV modules with ribbon or wire interconnection are often used as their production technology still prevails [11].

We therefore present an approach that makes the appearance of PV modules for integrative applications containing common PERC solar cells with five-busbar interconnection more homogeneous, while the long-term stability of the module remains unaffected. For this purpose, we develop an inkjet process that complies with the throughput of industrial stringers. We give details about the inkjet process, the optical impression of blackened cell strings in PV modules and how the electrical performance of the PV modules is influenced by our inkjet process.

2 EXPERIMENTAL

2.1 Inkjet Printing for Module Integration

The ink is applied using an industrial inkjet print head based on the continuous inkjet printing (CIJ) process [12]. Therefore, the print head is integrated into a printer platform, which allows movements in all spatial directions (x, y, z, rotation) via computer control. Three-cell strings from industrial monofacial M3 PERC half cells with five cell connectors (0.22 mm × 0.90 mm, Sn60Pb40 solder, industrial infrared soldering on stringer) are used to print on. An industrial inkjet ink based on butanone as solvent is used. The print pattern thus consists of five parallel stripes with a length of 245 mm (three half cells) and a pitch of 31.2 mm (busbar distance). The blackened width is approximately 1.4 mm to cover the vertical edges of the cell connectors and to compensate for the alignment tolerance of the stringer. In order to reduce the complexity of the multidimensional parameter field that affects droplet pitch (modulation frequency of the deflection voltage, jet frequency, printhead-substrate distance, etc.), the printing speed is varied at a fixed modulation frequency of the print head. A sufficient pitch of the droplets on the substrate is adjusted to fully cover the area without pinholes.

2.2 Module Manufacturing

The printed strings are cross-connected. The cross connectors themselves and the cell connectors protruding above the solar cell edges are not blackened in this experiment. Ethylene-vinyl acetate (EVA, 450 µm thickness) without UV cut-off for the front encapsulation and with UV cut-off at 350 nm for the rear encapsulation,

3 mm thick glass and a common black backsheet foil without diffusion barrier layer is used for encapsulation in an industrial laminator.

2.3 Climate Chamber Tests

We perform temperature cycling (TC) and damp-heat (DH) climate chamber tests twice following the IEC standard [13], and ultraviolet (UV) tests following IEC 61730 [14]. That means 400 cycles of TC without current applied, 2000 h exposure to DH, and 120 kWh/m^2 UV radiation. Additionally, we expose similar-built modules to combined tests: UV-DH (120 kWh/m^2) and UV-DH (120 kWh/m^2) followed by 200 thermal cycles, respectively. The IEC tests and the extended tests are performed with two modules containing three-cell-strings each. Two additional modules with inkjet printing and two modules without coating serve as reference. These reference modules are not subjected to ageing tests.

2.4 Module Characterisation

For PV module characterisation, we use three different methods. Scanning the modules is utilised to evaluate the optical impression of the modules initially as well as after passing the accelerated aging tests. We determine the electrical performance of our modules by means of *IV* measurements. Prior to each *IV* measurement, we illuminate the PV modules for 48 h to ensure comparability of the power measurements before and after the ageing processes [15]. Subsequently, we conduct electroluminescence (EL) based upon the determined short circuit currents (I_{SC}) of the modules by *IV* measurements of the modules. Our *IV* measurements show reproducibility within about 0.2 % in I_{SC}, 0.5 % in open circuit voltage (V_{OC}) and 0.7 % in maximum power point (P_{MPP}). The reproducibility for the fill factor (*FF*) measurements is about 1.4 %. Via error propagation, this results in a reproducibility of ± 0.4 % for I_{SC}, ± 1.4 % for P_{MPP}, and ± 2.8 % for *FF* in the relative plot of the *IV* parameters (*cf.* Figs. 4(a) and 6(a)).

3 RESULTS AND DISCUSSION

3.1 Inkjet Printing on Cell Connectors

In this experiment, we determine a sufficiently high droplet density on the surface of cell connectors and busbars using different droplet pitches so that the strings are homogeneously covered in black. The selected pitch of the droplets and the selected printing speed of 80 mm/s with a fixed modulation frequency of the deflection voltage result in a single droplet size of approximately 300 µm and a fully covered area without pinholes (*cf.* Fig. 1(a)). The variation of the printing speed of the print head shows that one cell connector of an M3 half-cell can be printed completely black within about one second in the CIJ process (*cf.* Fig. 1(b)). The inkjet process directly follows the stringing process, which itself thus remains unaffected: No influence on the soldering process and the resulting joints, no further damage of the coating on the cell connectors by additional handling steps within the stringer. In addition, the presented inkjet process blackens the areas of the busbars that are not covered by the cell connectors, because these usually end a few millimetres before the solar cell edge (*cf.* Fig. 1(b)).

We determined the maximum printing speed of our experimental setup to promote the integration of our CIJ process into industrial stringers (soldering process < 2 s per solar cell [16]). As a result, fully covered cell connectors without the appearance of pin holes or other printing defects on M3 cell level have been verified for a printing velocity up to 500 mm/s, limited by the axis system of the used printer platform. The specification of the used CIJ print head indicates a maximum print speed of 10 m/s. This is significantly higher than the typical process speeds of industrial stringers (up to about 6000 solar cells per hour [16]) and therefore does not represent a fundamental limitation.

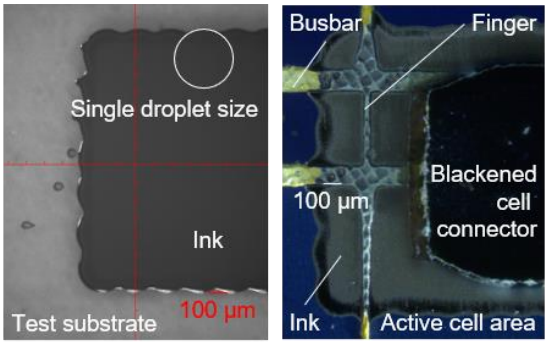

(a) (b)

Figure 1: (a) Printing at 80 mm/s with fixed modulation frequency of the deflection voltage on a test substrate and (b) on an interconnected solar cell. The single droplet size is approximately 300 µm. The selected pitch of the droplets results in a fully covered cell connector without pinholes.

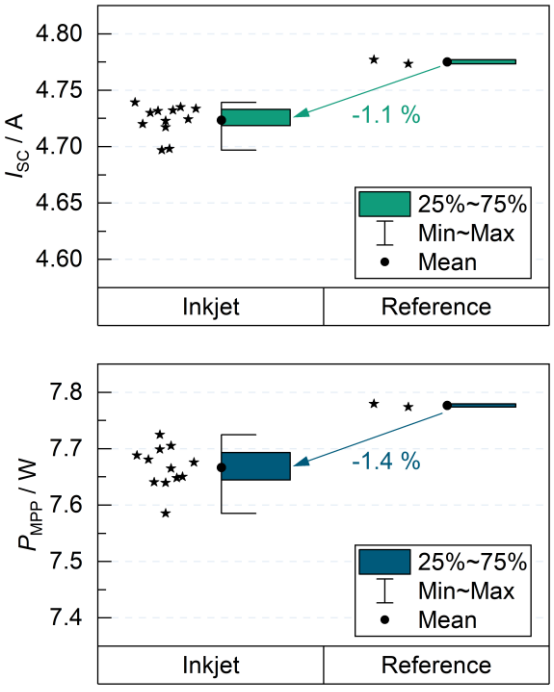

Figure 2: *IV* data of all PV modules after printing on the cell connectors and before climate chamber testing (left) and of the two reference modules without inkjet coating (right).

The initial *IV* data of all PV modules show the influence of the inkjet coating on I_{SC} and P_{MPP}. After printing and module integration of the solar cells, the I_{SC} decreases by 1.1 % ± 0.4 % and the maximum power drops by

1.4 % ± 1.4 %, respectively (*cf.* Fig. 2). The ink-covered surfaces as well as the edges of the cell connectors reduce or even prevent reflection of incident light onto the solar cell surface (*cf.* Fig. 3). We conclude that the selected ink has high opacity; attention must be paid to the print width when printing on the cell connectors to keep I_{SC} losses low but still cover the full connector because of alignment.

3.2 Optical Impression After Aging Tests

Figure 3 shows scans of PV modules in their initial state: (a) before TC test, (b) before UV test, (c) before DH test. The alignment tolerance of the stringer in combination with a narrow print width leads to partially visible busbars (*cf.* Fig. 3(a), (b)) and cell connectors (*cf.* Fig. 3(c)). Nevertheless, these images reveal the major

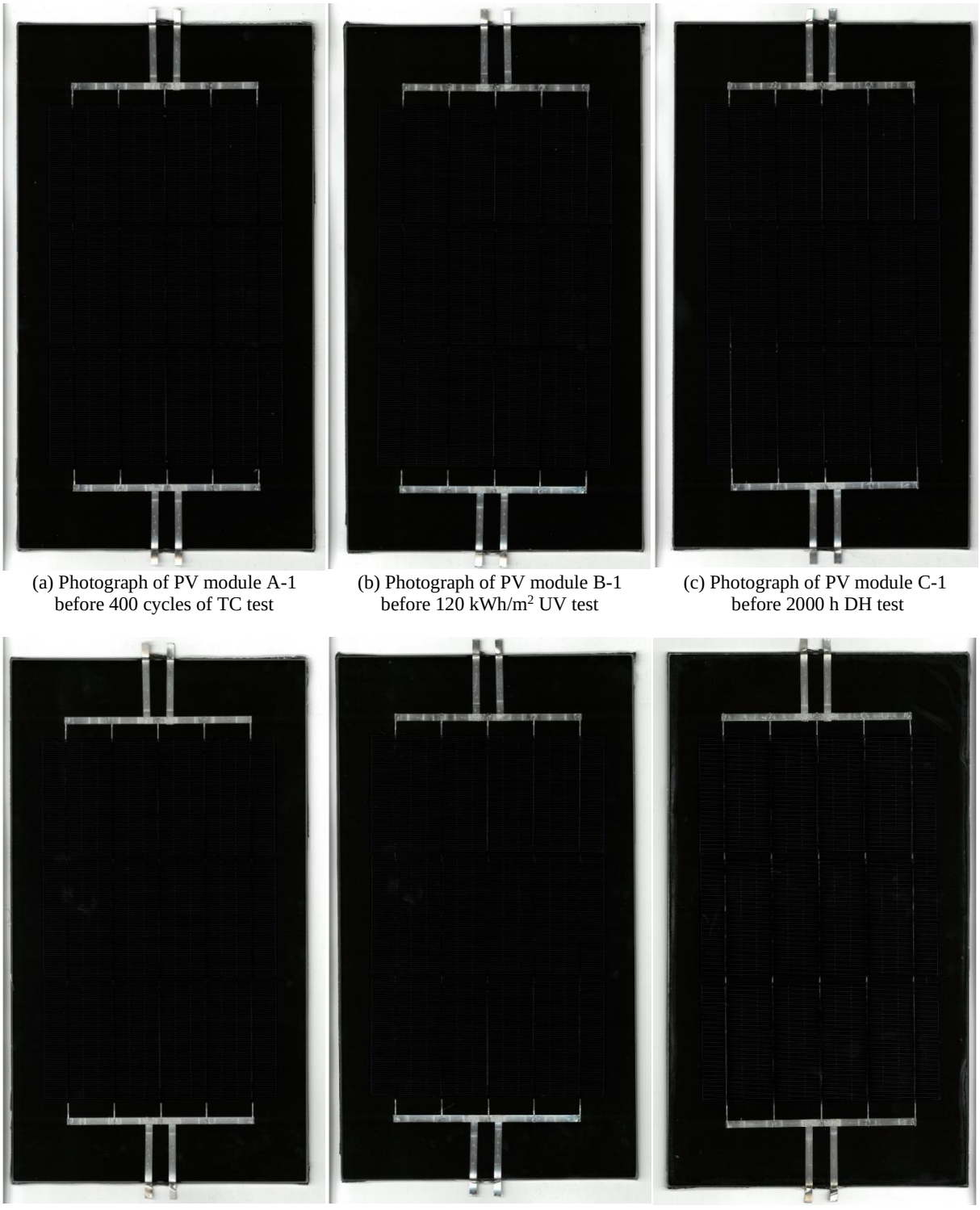

(a) Photograph of PV module A-1 before 400 cycles of TC test

(b) Photograph of PV module B-1 before 120 kWh/m^2 UV test

(c) Photograph of PV module C-1 before 2000 h DH test

(d) Photograph of PV module A-1 after 400 cycles of TC test

(e) Photograph of PV module B-1 after 120 kWh/m^2 UV test

(f) Photograph of PV module C-1 after 2000 h DH test

Figure 3: Three exemplary PV modules with inkjet-coated cell connectors in their initial state (a) to (c) and after the double climate chamber test runs according to the IEC standard (d) to (f).

advantage of the CIJ printing process: the pleasing homogeneous black appearance of the cell matrix in PV modules. Fig. 3(d) to (f) shows the same modules after ageing: (d) after 400 cycles of TC, (e) after 120 kWh/m^2 UV, (f) after 2000 h DH. Judging from the visual impression, which is of major importance for XIPV PV modules, a double TC test with 400 thermal cycles seems to have no effect on the stability of the inkjet-printed black coating. The results indicate that the ink coating has good thermomechanical properties; no cracking is visible. After the double UV test, there is also no visible deterioration of the black homogeneous impression. After 2000 h DH test, there is a minimal deterioration of the initial imperfect printing (*cf.* Fig. 3(f)). Especially in the cell gaps, the homogeneous coverage of the cell connectors seems to be reduced to some extent. This deterioration could be related to an interaction with acetic acid formed by the EVA during DH test [17, 18]. A different encapsulation material, which does not form acetic acid under humidity exposure, such as *e. g.* polyolefin (POE) could overcome this issue.

3.3. Module Characteristics After Two Times IEC Tests

Figure 4(a) shows the *IV* data of the PV modules that underwent the TC, UV and DH test procedures twice; each dot represents a tested module. The data are presented in relative form and refer to the initial values, which correspond to unity in the diagrams. Within the measurement uncertainty of the sun simulator, the I_{SC} almost remains constant. TC and DH test procedures seem to have an impact on the P_{MPP} of the PV modules and a minor impact on their *FF*.

However, the inkjet coating does not lower the PV module power after climate chamber tests. But rather certain defects that also occur in PV modules without printed cell connectors, as the EL images show (*cf.* Figs. 4(b) to (d)):

After 400 thermal cycles, finger failures occur because the cell connectors were not optimally aligned over the busbars in the stringing process, but were slightly soldered onto the fingers. As a result, the fine finger metallization tears off (*cf.* Fig. 4(b)). This defect can also be seen in PV modules without printed cell connectors [16]. We conclude that this is an issue of the busbar alignment to the cell but the coating has no influence on this. After UV radiation with 120 kWh/m^2 a dark area in the upper left corner of the top cell is visible. This is a typical error pattern for a faulty cross-connection [19]. After 2000 h

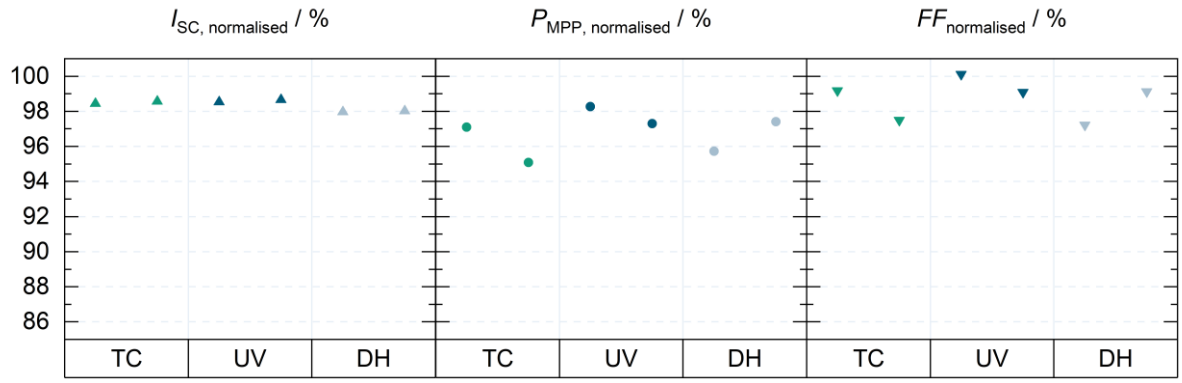

(a) *IV* data of PV modules after climate chamber tests twice following IEC standards. The measurement reproducibility is ± 0.4 % for I_{SC}, ± 1.4 % for P_{MPP}, and ± 2.8 % for *FF*.

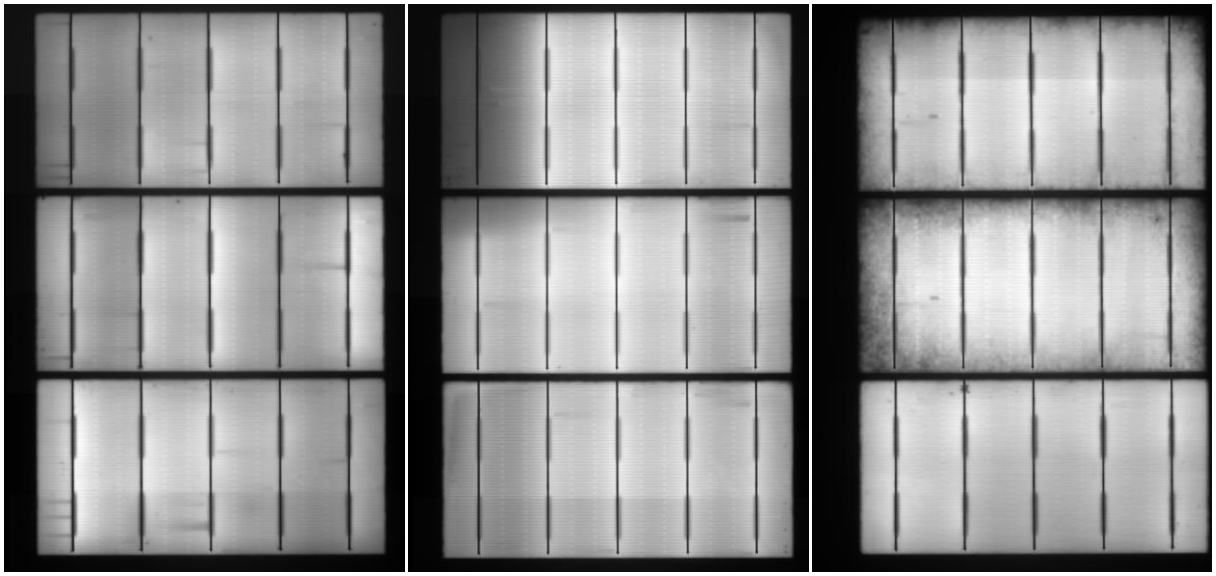

(b) EL image of PV module A-2 after 400 cycles of TC test

(c) EL image of PV module B-1 after 120 kWh/m^2 UV test

(d) EL image of PV module C-1 after 2000 h DH test

Figure 4: *IV* data of PV modules after climate chamber tests (a) and EL images of three exemplary PV modules with inkjet-coated cell connectors in their state after the double climate chamber test runs according to the IEC standards (b) to (d).

DH, the visual impression suffers due to coating degradation (*cf.* section 3.2). But cell defects are responsible for the power loss seen in the *IV* data: the inactive outer cell area of the middle cell, and less in the upper cell, is a typical defect of DH (*cf.* Fig. 4(d)) [18].

3.4 PV Module Performance After Combined Tests

The PV modules that were subjected to the combination of test procedures (UV-DH and UV-DH followed by TC) are shown in Figure 5. Judging from the visual impression, the combined test procedures have notable but little impact on the black appearance of the PV modules. As discussed in section 3.3, we ascribe the minimal deterioration of the homogeneous coverage of the cell connectors in the cell gaps to the influence of damp heat (*cf.* section 3.2). The degradation caused by the combined tests is more moderate. The visible effects are less severe than in the individual tests (*cf.* Fig: 6(b), (c)).

The *IV* data along with the EL images of these modules are displayed in Figure 6. The combined climate chamber tests neither significantly degrade the I_{SC}, P_{MPP} nor the *FF* (*cf.* Fig. 6(a)) and the typical failure modes as described in section 3.4 are visible as a combination in the EL images (*cf.* Fig. 6(b) and (c)). This is particularly clear in Fig. 6(c), where DH and TC induced defects appear together: tear off of finger metallization, faulty cross-connection, and inactive outer cell area.

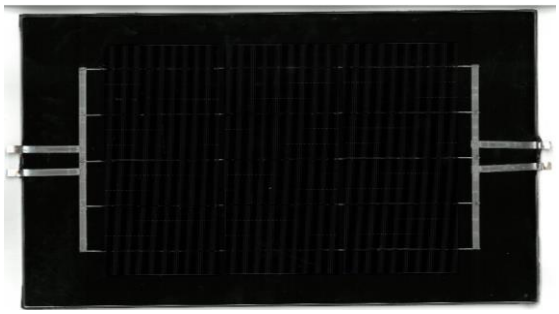

(a) Photograph of PV module D-1 after the combined UV-DH test (120 kWh/m^2).

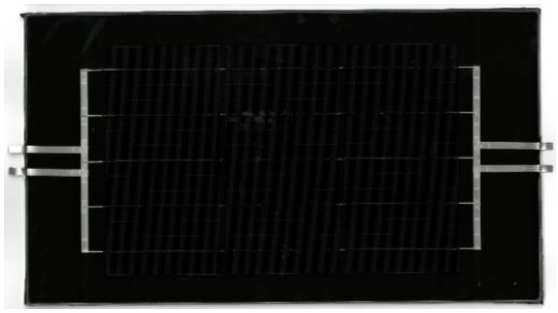

(b) Photograph of PV module E-1 after the combined test UV-DH (120 kWh/m^2) followed by TC 200.

Figure 5: Two exemplary PV modules with inkjet-coated cell connectors after the combination of test procedures UV-DH (a) and UV-DH followed by TC (b).

4 CONCLUSIONS

To reach the 7th goal of the sustainable development goals, a strong expansion of photovoltaics is inevitable. To use all available areas, integrated PV is a key technology. An appealing design of PV modules promotes acceptance.

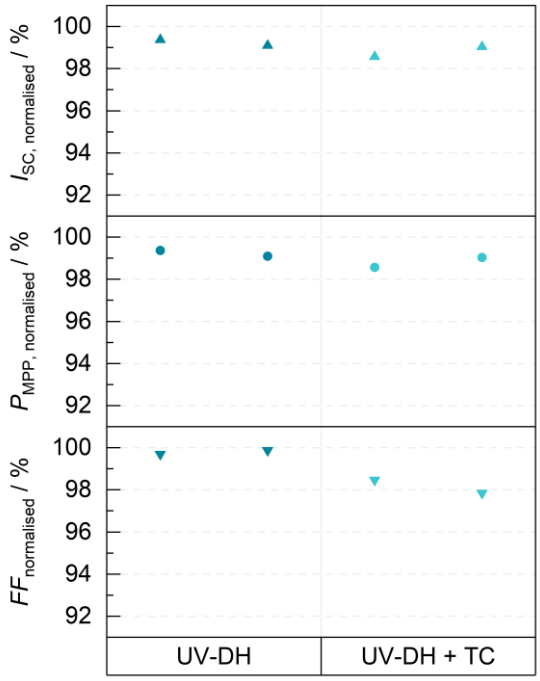

(a) *IV* data of PV modules with inkjet-coated cell connectors after the combination of test procedures UV-DH and UV-DH followed by TC and of the four reference modules. The reproducibility is ± 0.4 % for I_{SC}, ± 1.4 % for P_{MPP}, and ± 2.8 % for *FF*.

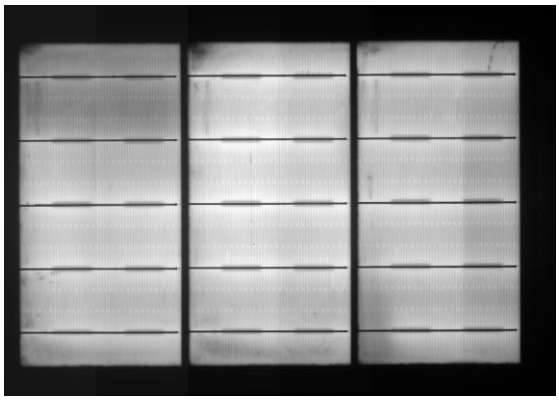

(b) EL image of PV module D-1 after the combined test UV-DH (120 kWh/m^2).

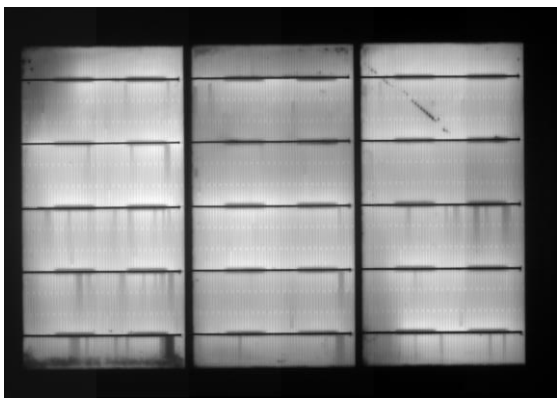

(c) EL image of PV module E-1 after the combined test UV-DH (120 kWh/m^2) followed by TC 200.

Figure 6: *IV* data of PV modules after the combination of test procedures (a) and EL images of the two exemplary PV modules with inkjet-coated cell connectors (b) and (c).

Our CIJ process to blacken cell connectors for homogeneous black appearing PV modules is a promising approach for XIPV. The presented inkjet process results in homogeneous black PV modules while maintaining a high photoconversion efficiency and thus promotes the acceptance of integrated PV by a fast and easy coating process. This uniform optical impression remains constant after 400 thermal cycles, after 120 kWh/m^2 UV radiation exposure and is only slightly affected by 2000 h of DH and the combined climate chamber tests (*cf.* Fig. 7).

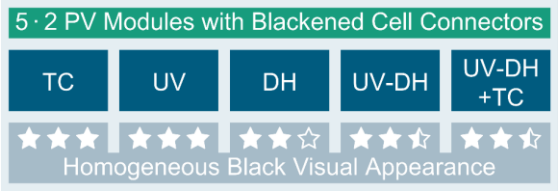

Figure 7: Summing up flow chart of the investigated PV modules with inkjet coated cell connectors.

The relative losses in I_{SC} and P_{MPP} of the PV modules due to blackening the cell connectors are about 1.1 % and 1.4 %, respectively. The used industrial inkjet ink is stable after 400 cycles of TC and after 120 kWh/m^2 of UV radiation exposure. The homogeneous coverage of the cell connectors only shows a minor deterioration after 2000 h of DH and the combined tests where DH was applied. The visual deterioration was observed in the cell gaps and may be related to an interaction with acetic acid formed by the EVA during DH test. Another encapsulation material which does not form acetic acid may overcome this issue.

We observed degradation during ageing tests, however the observed degradation mechanisms could all be explained by expected defect patterns that also occur in modules without inkjet coating of the cell connectors. Therefore, we conclude that these are responsible for the lower performance of the PV modules after climate chamber tests.

The continuous inkjet process, presented for blackening the cell connectors on solar cells directly follows the string production, which itself remains unaffected: No influence on the soldering process and the resulting joints, no further damage of the coating on the cell connectors by additional handling steps within the stringer. The specification of the used CIJ print head indicates a maximum print speed of 10 m/s. This is significantly higher than the typical process speeds of industrial stringers. With this and the parallelization of multiple print heads, the CIJ process can be easily adapted to the throughput of PV module production lines. The print width variability also allows an adaption for cells with multiple busbars or wires.

However, a detailed analysis of costs for integrating the CIJ process into existing PV module production lines is still pending. For full-size black PV modules, the cross connectors have to be blackened as well. Depending on the module topology, i.e., the number and positions of the cross-connectors, this presents yet another challenge.

5 ACKNOWLEDGEMENTS

This work was funded by the German Federal Ministry for Economic Affairs and Climate Action under the contract numbers 03EE1049A (PV-Hide).

6 REFERENCES

[1] D. H. Meadows, D. L. Meadows, J. Randers, and W. W. Behrens, *The limits to growth: A report for the Club of Rome's Project on the Predicament of Mankind*, 2nd ed. New York: Universe Books, 1974.

[2] *Paris Agreement*, 2016. [Online]. Available: https://treaties.un.org/Pages/ViewDetails.aspx?src=IND&mtdsg_no=XXVII-7-d&chapter=27&clang=_en

[3] Untied Nations, "Transforming our world: the 2030 Agenda for Sustainable Development: Resolution adopted by the General Assembly on 25 September 2015. Seventieth session, Agenda items 15 and 116," A/RES/70/1, Oct. 2015. [Online]. Available: https://www.refworld.org/docid/57b6e3e44.html

[4] J. Brandes, M. Haun, D. Wrede, P. Jürgens, C. Kost, and H.-M. Henning, "Wege zu einem klimaneutralen Energiesystem: Die deutsche Energiewende im Kontext gesellschaftlicher Verhaltensweisen," Update November 2021: Klimaneutralität 2045, Fraunhofer-Institut für Solare Energiesysteme ISE, Freiburg im Breisgau, Nov. 2021. Accessed: Jun. 24 2022. [Online]. Available: https://www.ise.fraunhofer.de/content/dam/ise/de/documents/publications/studies/Fraunhofer-ISE-Studie-Wege-zu-einem-klimaneutralen-Energiesystem-Update-Klimaneutralitaet-2045.pdf

[5] H. Wirth *et al.*, "Integrierte Photovoltaik: Aktive Flächen für die Energiewende," FVEE Themen 2019 Aktuelle Forschungsfragen - Integrierte Photovoltaik, 2020. [Online]. Available: https://www.google.com/url?sa=t&rct=j&q=&esrc=s&source=web&cd=&ved=2ahUKEwj5nJSWruT5AhUF-qQKHckOB7sQFnoECBAQAQ&url=https%3A%2F%2Fwww.fvee.de%2Fwp-content%2Fuploads%2F2022%2F01%2Fth2019_03_01.pdf&usg=AOvVaw0tJA04bC7GUCGu-6dUINhb

[6] C. Kutter *et al.*, "Decorated Building-Integrated Photovoltaic Modules: Power Loss, Color Appearance and Cost Analysis," 2018, doi: 10.4229/35THEUPVSEC20182018-6AO.8.6.

[7] T. E. Kuhn, C. Erban, M. Heinrich, J. Eisenlohr, F. Ensslen, and D. H. Neuhaus, "Review of Technological Design Options for Building Integrated Photovoltaics (BIPV)," *accepted for publication in the Energy and Buildings special issue review articles from the editors*, 2020.

[8] B. Bläsi, T. Kroyer, T. Kuhn, and O. Höhn, "The MorphoColor Concept for Colored Photovoltaic Modules," *IEEE Journal of Photovoltaics*, vol. 11, no. 5, pp. 1305–1311, 2021, doi: 10.1109/JPHOTOV.2021.3090158.

[9] A. Morlier *et al.*, "Photovoltaic Modules with the Look and Feel of a Stone Façade for Building Integration," *Sol. RRL*, vol. 6, no. 5, p. 2100356, 2022, doi: 10.1002/solr.202100356.

[10] N. Klasen, D. Weißer, T. Geipel, D. H. Neuhaus, and A. Kraft, "Performance of Shingled Solar Modules Under Partial Shading," *Progress in Photovoltaics: Research and Applications*, 2021, doi: 10.1002/PIP.3486.

[11] ITRPV, "International Technology Roadmap for Photovoltaic (ITRPV): 13th edition, 2021 Results," 2022. [Online]. Available: https://www.vdma.org/international-technology-roadmap-photovoltaic

[12] G. Cummins and M. P. Desmulliez, "Inkjet printing of conductive materials: a review," *Circuit World*, vol. 38, no. 4, pp. 193–213, 2012, doi: 10.1108/03056121211280413.

[13] *DIN EN IEC 61215-2 Terrestrial photovoltaic (PV) modules – Design qualification and type approval – Part 2: Test procedures*.

[14] *Photovoltaic (PV) module safety qualification – Part 2: Requirements for testing*, IEC 61730-2:2016, International Electrotechnical Commission (IEC), Geneva, Switzerland, 2016.

[15] A. A. Brand *et al.*, "Ultrafast in-line capable regeneratrion process for preventing light induced degradation of boron-doped p-type Cz-silicon PERC solar cells," in *33rd EU PVSEC*, Amsterdam, The Netherlands, 2017. Accessed: Jul. 4 2019. [Online]. Available: https://www.ise.fraunhofer.de/content/dam/ise/de/documents/publications/conference-paper/33-eupvsec-2017/Brand_2CO95.pdf

[16] A. De Rose, "Evaluation of solder joints on aliminum surfaces for the interconnection of silicon solar cells," Dissertation, Universität Rostock, Rostock, 2021.

[17] I. Duerr, C. Peike, S. Hoffmann, M. Koehl, and K.-A. Weiß, "X-ray study on the damp-heat induced cell degradation (DHID)," in *Proceedings of the 28th European Photovoltaic Solar Energy Conference and Exhibition*, Paris, France, 2013, pp. 3300–3302.

[18] C. Peike *et al.*, "Origin of damp-heat induced cell degradation," *Sol Energ Mat Sol C*, vol. 2013, pp. 49–54, 2013.

[19] M. Köntges, S. Kurtz, C. Packard, U. Jahn, K. A. Berger, and K. Kato, *Performance and reliability of photovoltaic systems: Subtask 3.2: Review of failures of photovoltaic modules : IEA PVPS task 13 : external final report IEA-PVPS*. [Sankt Ursen]: International Energy Agency, Photovoltaic Power Systems Programme, 2014.